The Ultraboost Extreme Downsizing Project: Direct Injection, Compound Charging, Variable Valve Timing and 60% Less Capacity

Dr. James **Turner**, Andrew **Popplewell**, Steve **Richardson**
Jaguar Land Rover, Coventry, UK

Andrew **Lewis**, Dr Sam **Akehurst**, Dr Chris **Brace**, Dr Colin **Copeland**
University of Bath, Bath, UK

Summary

The paper presents results from Ultra Boost for Economy, a collaborative project which aims to achieve the torque curve of a modern, high-specification 5.0 litre naturally-aspirated engine from a highly-boosted 2.0 litre engine, while encompassing the necessary mechanical attributes to employ such a concept in premium vehicles. The main purpose of this project was to show that the engine could, in itself, provide most of a 35% reduction in vehicle tailpipe CO_2 emissions when measured on the New European Drive Cycle. The performance targets included achieving 32.4 bar BMEP at 3500 rpm, 142 kW/litre (190 bhp/litre) at 6500 rpm and 25.1 bar BMEP at 1000 rpm.

Previous papers have reported performance data without the engine-driven charging system, instead using advanced boosting and EGR supply rigs. This earlier work demonstrated the capability of the combustion system to perform to the required standard without the potentially complicating effect of a novel charging system being fitted. The present work provides a status of the full-load performance and part-load economy results gathered from the engine when operating with a near-final specification of the fully-functioning and self-contained engine-driven charging system. The results demonstrate the potential for the full torque curve to be successfully met, together with how the downsizing potential promises to deliver significant fuel consumption improvements in the vehicle. A preliminary result from a proprietary vehicle fuel consumption model is also included to show this, which also illustrates the continued importance of low idle fuel consumption towards low drive-cycle fuel economy as rated on the New European Drive Cycle, even in heavily-downsized engine applications.

1 Introduction

Engine downsizing has become firmly established in the automotive industry as providing an affordable solution to reduce tailpipe CO_2 and improve fuel economy. It also potentially provides improved driveability from gasoline engines in the form of

lower peak torque speeds (or the 'knee point' in a typical turbocharged engine torque curve), which in turn allows downspeeding. To the OEM, the attractions of a downsizing strategy include that gasoline engine technology is very cost-effective to produce versus diesel engines (especially when the costs of the exhaust after treatment (EAT) system are included), that there are still significant efficiency gains to be made in such engines due to the inherent losses associated with the four-stroke cycle, and that pursuing the technology does not entail investing in completely new production facilities (as would be required by a quantum shift to electric or fuel-cell vehicles, for example).

The advantages of downsizing a 4-stroke Otto cycle spark-ignition (SI) engine arise from shifting the operating points that the engine uses in its map for any given flywheel torque, so that the throttle is wider-open, which provides reduced pumping losses. At the same time, the mechanical efficiency increases, being defined as

$$\eta_{\text{mech}} = \frac{\overline{p}_{\text{brake}}}{\overline{p}_{\text{ind}}} \ , \qquad \text{Eqn 1}$$

where η_{mech} is the mechanical efficiency, $\overline{p}_{\text{brake}}$ is the brake mean effective pressure (BMEP) and $\overline{p}_{\text{ind}}$ is the gross indicated mean effective pressure (IMEP) [1]. Thermal losses also improve and, in the case of downsizing and decylindering from a Vee-configuration engine to an in-line one, crevice volume losses can be reduced and there are potentially significant savings in bill of materials (BOM) and manufacturing costs, too.

On a vehicle level the increased number of ratios in new automatic transmissions, and with them the ability to provide an increased ratio spread, permits the consequent rematching of the transmission which further improves vehicle fuel consumption. For any given flywheel power, selecting a higher ratio and downspeeding the engine moves it to higher loads at lower speeds, where friction is generally less, thus further improving the mechanical efficiency and reducing pumping losses. At the same time, more-complex electronic powertrain controls provide the excellent driveability that the customer has become accustomed to. This illustrates the important contribution non-engine technologies can give, especially if aerodynamic and driveline frictional losses can be improved at the same time.

The savings implicit in down-cylindering (and if possible changing the configuration of the engine to reduce the number of cylinder banks) can help to offset any additive technologies found necessary to recover the power output necessitated by the vehicle application and its required performance. To do this pressure charging, usually in the form of turbocharging, is generally adopted since it allows a degree of recovery of energy from the exhaust gas. There are significant synergies with other commonplace technologies such as direct injection (DI) and camshaft phasing devices, too [2].

The ‘downsizing factor’ of such engines is here defined to be

$$DF = \frac{V_{Swept_{NA}} - V_{Swept_{Downsized}}}{V_{Swept_{NA}}}, \qquad \text{Eqn 2}$$

where DF is the downsizing factor, $V_{Swept_{NA}}$ is the swept volume of a naturally-aspirated engine of a given power output and $V_{Swept_{Downsized}}$ is the swept volume of a similarly-powerful downsized alternative.

To date what may be considered to be *DFs* in the region of up to 40% have been used in production [3,4] and up to 50% has been shown in research engines [5]. At the time that the Ultraboost project started, such engine concepts did not seem to have reached the limit of the technology, so in order to try to ascertain what is ultimately possible with the approach, the project was formed with the major tasks of specifying, designing, building and operating an engine with a *DF* of at least a 60%. It also aimed to inform whether such a level of downsizing could provide a route to a 35% reduction in tailpipe CO_2 on the New European Drive Cycle (NEDC), with a Stop/Start system being used but no other forms of hybridization. Extremely high low-speed BMEP was also a target, higher than is typically shown by conventional downsizing concepts, in order to assess further downspeeding opportunities.

To provide a valid reference for premium vehicles, a prime aim of the project was to reproduce the power and torque curves of the Jaguar Land Rover 5.0 litre AJ133 naturally-aspirated V8 engine. The AJ133 NA engine produces 515 Nm at 3500 rpm, 283 kW (380 bhp) at 6500 rpm and 400 Nm at 1000 rpm, a wide torque curve for a NA engine being facilitated by extra technology in the form of wide-range dual continuously-variable camshaft phasing (DCVCP) devices and cam profile switching (CPS) tappets [6]. Adopting a DF of 60% implied that a pressure-charged engine with a maximum of 2.0 litre capacity [7,8] would be required, and that the ensuing BMEP targets for a pressure-charged engine would be extremely challenging; effectively this meant achieving minimum BMEPs of 32.4 bar, 26.1 bar and 25.1 bar at the peak torque, peak power and 1000 rpm respectively. The latter value would be a stern test for both the combustion and charging systems, which led to a novel approach to the way in which the project was conducted, as discussed briefly below.

2 Partners and phases of the Ultraboost project

The Ultraboost project commenced September 2010 for a duration three years and comprised eight partners. Since it is pertinent to the discussion of the latest results, the individual partner’s contributions are discussed in brief below, with further detail on the project and its structure being provided in [8]. The general partner responsibilities were:

Jaguar Land Rover was the lead partner, with responsibility for engine build, general procurement, engine-mounted charging system integration and overall project management.

GE Precision Engineering provided engine design and machining capabilities as well as background knowledge on the design of high-specific-output racing engines.

Lotus Engineering provided a dedicated engine management system (EMS), 1-D modelling and know-how on pressure-charged engines, and support for engine testing.

CD-adapco supported the design process with steady-state and transient CFD analysis primarily in order to support intake port design.

Shell provided test fuels and autoignition know-how.

The University of Bath conducted all of the testing, having dedicated boosting and cooled exhaust gas recirculation (EGR) rig which were used for the initial Phase 2 testing of the demonstrator engine (see below).

Imperial College London specified the charging system components, with support from both JLR and Lotus, and tested them in order to characterize them accurately so that the 1-D model was as robust as possible.

The University of Leeds developed their autoignition model to assist with the 1-D modelling process.

The project was conducted in three phases, in turn divided into different work packages. In Phase 1, a production JLR 5.0 litre AJ133 V8 engine was commissioned and had its performance, emissions and fuel economy baselined on the test bed. As a next step, the Denso engine management system (EMS), which was used in production then, was replaced by the Lotus EMS. This was shown to be capable of fully controlling the engine and giving exactly the same results at full and part load, including matching the steady-state fuel consumption of the production EMS to ≤ 0.5%. This phase therefore set the fuel consumption benchmarks for the project's downsized engine design and proved the capability of the Lotus EMS when controlling a direct-injection engine with many high-technology features, including the use of multiple-injection strategies.

In parallel with the Phase 1 engine test work, Phase 2 specified, designed and procured the core Ultraboost engine (known as UB100). To do this the pooled knowledge of all the parties was used, resulting in a current industry best-practice high-BMEP engine with some additional novel features. Once Phase 1 testing had been completed, the AJ133 removed and the UB100 engine commissioned at Bath, the Phase 2 test programme commenced. This utilized a test bed combustion air handling unit (CAHU) together with a specially-designed EGR rig to pump EGR gas up to the pressure of the plenum. This was necessary despite the fact that the final

engine, with its self-driven charging system, was to use low-pressure EGR, since it was not acceptable for the CAHU unit to flow EGR gas.

Phase 2 testing was primarily intended to prove out the capability of the newly-developed combustion system. It also permitted fuel testing to be undertaken without the complicating effects of an engine-driven charging system. However, this important subsystem would also be specified, modelled, procured and validated in a parallel work stream within this phase.

Phase 3 was intended to comprise any redesign of the UB100 engine which was found to be necessary during Phase 2 testing coupled with mounting the self-driven charging system to UB100. The engine was then to be known as UB200 and tested to provide data to help establish the level of achievement of the project targets. Ultimately this will be demonstrated by a combination of direct measurement of results from the UB200 engine on the test bed (for power, torque, driveability etc.) and by subsequent modelling (by the application of minimap fuel consumption data gathered to a current JLR vehicle performance model, this being necessary since the baseline AJ133 engine is no longer fitted to the target vehicle). CO_2 emissions improvement will also be shown in this vehicle modelling work, the results of which will be reported at a later date.

3 Overview of UB200 engine design

The details of the Ultraboost engine design, and how it was derived from the Jaguar Land Rover AJ133 engine, have been discussed in earlier work [8]. This also detailed the modifications to the UB100 level to create the UB200 level with its self-driven charging system, specified in parallel and discussed in detail in [9]. As a consequence it is not intended to describe the engine in detail here: an overview will be provided instead.

From preliminary work, and in line with the downsizing ambitions described above, the engine was specified as a 2.0 litre in-line 4-cylinder with central close-spaced direct injection, compound pressure charging, variable valve timing and 60% less capacity than the AJ133 baseline engine. The general specifications of the engine are listed in the table shown in Figure 1. The injection orientation is of the ‘asymmetric’ type, with the plane containing the spark plug and injector parallel to the crankshaft axis.

From the data in Figure 1 the undersquare nature of the engine is readily apparent. This characteristic was specifically chosen to provide a small bore to help shorten the flame travel across the combustion chamber, in turn to benefit the knock limit, to reduce thermal losses and also to benefit the engine’s resistance to preignition.

While the exact causes of the type of preignition currently providing a limit to 4-stroke downsizing are presently the subject of intense research at the moment, they are

believed to include oil being ejected from the top land and subsequently autoigniting during the compression stroke. In turn this ignites the main body of the charge [10,11,12]. Consequently, because of the relationship between bore diameter and top land area, adopting a small bore diameter is directionally correct.

CAD images of the engine in UB200 form are shown in Figure 2.

General architecture	4-cylinder in-line Four valves per cylinder
Construction	All-aluminium AJ133 cylinder block converted to single-bank operation with the A Bank (right-hand side) Siamesed liner pack to facilitate reduced bore diameter Dedicated cylinder head
Bore	83 mm
Stroke	92 mm
Swept volume	1991 cc
Firing order	1-3-4-2
Combustion system	Pent-roof combustion chamber with asymmetric central direct injection and spark plug High-tumble intake ports Auxiliary port-fuel injection Secondary spark plug position possible in the under-intake-port location
Compression ratio	9.0:1
Valve gear	Chain-driven double overhead camshafts with fast-acting dual continuously-variable camshaft phasers (DCVCP) Cam profile switching (CPS) tappets used on inlet and exhaust
Charging system	Low-pressure stage: Garrett GT30 turbocharger with separate wastegate Inter-stage off-engine charge air cooler High-pressure stage: clutched Eaton R410 supercharger with overall 5.6:1 drive ratio (later changed to 5.9:1 - see text) Engine-mounted water-cooled charge air cooler Supercharger bypass
EGR system	Off-engine low-pressure loop configuration
Engine management system	Lotus ‘Euro 8’ ECU

Fig. 1: Ultraboost UB200 engine specification

Effectively, the engine is the A bank (or right-hand bank) of a heavily-modified AJ133 V8, with a new bore and stroke, a flat-plane crankshaft and attendant new firing order. This approach was taken because the bearings and scantlings of the AJ133 engine would be easily capable of handling the performance, since it is

offered in the market in ratings up to 542 bhp. The compound charging system was the subject of a great deal of research [9] and in terms of the general flow path comprises a Garrett GT30 turbocharger, an off-engine charge air cooler (CAC), a clutched Eaton R410 supercharger (intended to be driven at an overall ratio of 5.6 to the crankshaft, including an internal step-up gear ratio of 2.037:1, but see further comments in Section 6) and finally an engine-mounted water-cooled CAC feeding vertically into a small plenum. Additionally, there is a large bypass for the supercharger for when it is not engaged.

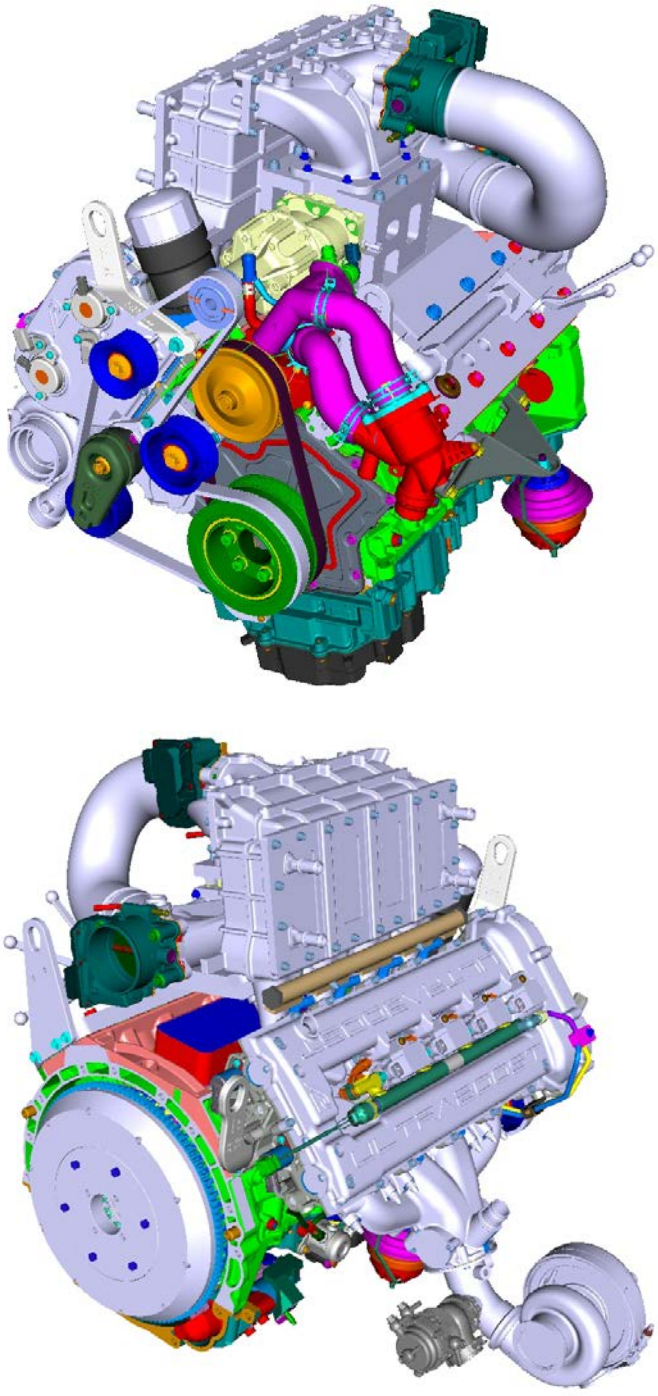

Fig. 2: CAD images of Ultraboost UB200 engine

The top part of Figure 2 shows the supercharger drive system together with the supercharger bypass and its throttle. The clutch on the Eaton R410 supercharger is visible between the drive pulley and the supercharger body, which itself is bolted vertically to a carrier from which a discharge duct connects to the water-cooled CAC. The plate which closes off the B bank water jacket in the AJ133 cylinder block is also visible and above this the pipe and valves which allow balancing of cooling system pressures in the absence of the B bank cylinder head can be seen. The bottom part of the figure shows the engine from the other side, including the water-cooled exhaust manifold (WCEM) (see below) and the Garrett GT30 turbocharger with its externally-mounted wastegate. The main load control throttle is also visible, from behind of which the bypass duct leads to the bypass throttle. Two production-derived water-cooled CAC blocks are used, configured in parallel, and their water inlet and outlet stubs can be seen on either end of the of the CAC housing. Finally, the PFI fuel rail can be seen beneath the plenum volume.

The engine was designed to withstand peak cylinder pressures of 130 bar, with known further countermeasures should it be considered advantageous to increase this to a greater level at a later date (for instance, when investigating high-octane fuels). The aluminium alloy piston itself is safe to 145 bar for the sort of duty cycle a research engine is used for.

The EMS was configured to be capable of controlling the many functions of the base engine as detailed in Figure 1, and ultimately also the selected charging system components, including the supercharger clutch and bypass [6]. It also permitted the investigation of strategies to help to address the large referred inertia of the supercharger and its effect on driveability (while its inertia of the supercharger itself is low, when multiplied by the high drive ratio to the crankshaft, the overall effect is large). These include ‘windmilling’ of the supercharger while it is clutched out by closing the bypass. Such an approach increases the pumping work of the engine, but does allow a significant proportion of the ‘closed clutch’ supercharger speed to be achieved therefore reducing the differential speed between pulley and shaft during a transient load step.

As mentioned, a WCEM was used. This is because while the integrated exhaust manifold (IEM) is becoming a common technology for production engines [13,14], and is particularly advantageous in turbocharged engines since it allows the removal of a large degree of component protection over-fuelling at high load [2,15], unfortunately, because of the bore and cylinder head bolt spacings necessarily inherited from the AJ133 engine, it was not feasible to design an IEM into the Ultraboost cylinder head. However, there was an interest in investigating a WCEM from the point of view of assessing full-load heat rejection, and it allowed a more advantageous exhaust path geometry than that of the log manifold originally specified and used in the UB100 testing in Phase 2, and mitigated the fact that the original’s outlet geometry was restrictive. It also permitted the provision of a flow splitter which could separate all the cylinders completely, pulse-divide cylinders 1 and 4 from 2 and 3, or permit full mixing (all at the entry to the turbine). The final design is

shown in Figure 3, in the left-hand side of which the flow splitter can be seen. Its water jacket is shown in the right-hand side of this figure; water flows from a distribution manifold below the individual feeds, combines within the jacket and then flows out through the single pipe on the top near to the gas outlet.

Fig. 3: Water-cooled exhaust manifold (WCEM)

Because of the importance of intake port geometry with respect to outright performance and to mixture preparation, at the outset of the project significant effort was directed at obtaining the best possible intake port. The following section discusses how this was obtained and performance it gave.

4 Intake port design and performance

For DISI engines there has been a general evolution towards high-tumble intake ports. This has been in order to achieve the necessary air motion to ensure the best possible mixture preparation at the time of ignition. The trend was synergistic with early under-port injector positions and the initial intention with DI to provide stratified lean operation as a fuel consumption enabler in naturally-aspirated engines. However, as the challenges of lean feed gas EAT became apparent in these early DI engines the situation became less attractive because of the reduction in flow capacity caused by the need to lift the port to clear an under-port injector position. In comparison, port fuel injection (PFI) engines did not require anywhere near the tumble rates of DI engines to achieve homogenization of the charge.

Realization of the synergy between DI and pressure charging, however, caused the move towards downsizing [16,17]. This was because in no small part the adoption of pressure charging helped to overcome the flow loss generally associated with high tumble intake ports, leaving the ability to maximize utilization of the latent heat of vaporization of the charge. The further adoption of variable valve timing, together with the ability of DI to delay fuel introduction until after the overlap phase had finished, enabled scavenging strategies to be adopted which pushed low-speed torque and driveability to levels significantly above that achievable with boosted PFI engines, to the benefit of downspeeding and downsizing, respectively.

While under-port placement of the injector had a symbiotic relationship with this evolution of the general port configuration of DISI engines, nevertheless the situation has arisen that reduced absolute port flow rate is seen as a worthwhile trade for increased tumble (and hence improved mixture preparation and charge cooling). For Ultraboost, because of the high BMEP rates and specific power targeted by the project, it was especially important to improve in this area of engine design over the current state of the art in order to provide high air flow rates with reduced charge cycle (pumping) work.

While it is accepted that it is of primary importance to have high charge motion near to top dead centre (TDC) when the spark is initiated, high tumble has another function earlier in the cycle as a means to homogenize the air, fuel, residual gases, oil droplets and temperature as fully as possible. Near to TDC piston geometry has an important effect with regard to the bulk flow breakdown and the generation of microturbulence, but during the intake stroke the importance of piston geometry gradually lessens towards bottom dead centre (BDC). Thus intra-cycle CFD should be employed to determine the best overall engine geometry but the air flow rig can be used as a good differentiator early in the port development process. This section briefly discusses how this process was followed within the project and compares the performance of the adopted port with a current production turbocharged DISI engine benchmark, the BMW N20 2.0 litre I4.

Although the N20 engine is rated at a BMEP level significantly below that which Ultraboost was targeting [18], it was still considered to be the current state-of-the-art in terms of specific power, BMEP and the fact that it had a central DI combustion system employing a multi-hole solenoid injector.

For the process adopted, a target was agreed upon based upon the JLR engine database and the knowledge of the other partners. Several ports were then designed which fitted the cylinder head package. With these ports designed, CD-adapco then brought their capabilities to bear in two distinct stages of the process: a first calculation stage where the steady-state flow characteristics were determined, and a second one where full transient calculations were carried out.

During the first part of this process 20 different ports were designed and analyzed under steady-state conditions. Filtering these led to five being chosen and carried forward to the second transient analysis stage. Finally one port design was selected and machined into the first UB100 cylinder head, with the other available heads being held back from machining should it be found necessary to implement any changes as a result of engine performance testing.

After the design had been chosen and the first head machined, the ports were flow tested on Lotus Engineering’s cylinder head air flow rig. These results were compared to data from the BMW N20 2.0 litre I4 engine which had also been measured on the same rig. The results of this flow rig testing are shown in Figures 4 to 6 and are discussed below.

Figure 4 presents the outright flow capability of the inlet port in comparison with the BMW engine. The Ultraboost flow at its maximum valve lift of 10.5 mm is 182 cubic feet per minute (CFM), and that for the BMW at a similar lift/throat diameter ratio is 139 CFM. Figure 5 shows the related flow coefficients, with Ultraboost having 0.633 and the BMW 0.520 at the same 10.5 mm valve lift condition. From this it can be seen that the port flow performance of Ultraboost in comparison to the N20 is extremely good, despite Ultraboost having a 1 mm smaller bore diameter. Part of this increased flow will be due to the 5.9% larger throat area of Ultraboost, but this does not account for the fact that the Ultraboost port flows nearly 30% more air than that of the N20 at 10.5 mm valve lift.

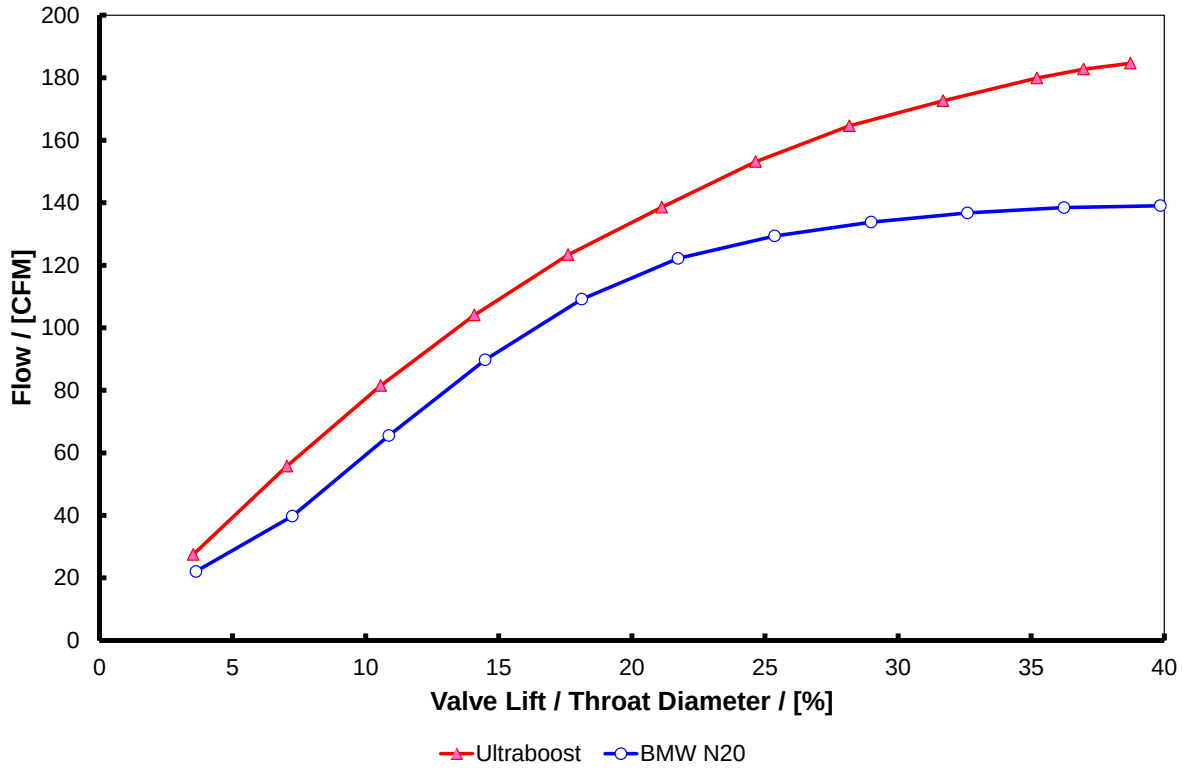

Fig. 4: Inlet port flow comparison for the Ultraboost Phase 2 and the BMW N20 cylinder heads

A comparison of non-dimensional tumble number is made in Figure 6. The N20 offers significantly higher tumble at low lift, employing valve shrouding in order to increase tumble in that area of the curve. This is a specific requirement because of its use of Valvetronic mechanically-variable valve train to minimize part-load throttling loss [18]. Since valve lift and duration are the primary means of controlling load while minimizing throttling loss with this system, its use makes it especially important to generate high tumble rates at low valve lifts: the high lift area of the curve is not used much in normal driving at all. Because of this a compromise in terms of reduced high-load activity in order to achieve greater rates at low load is presumably considered acceptable for the N20 engine.

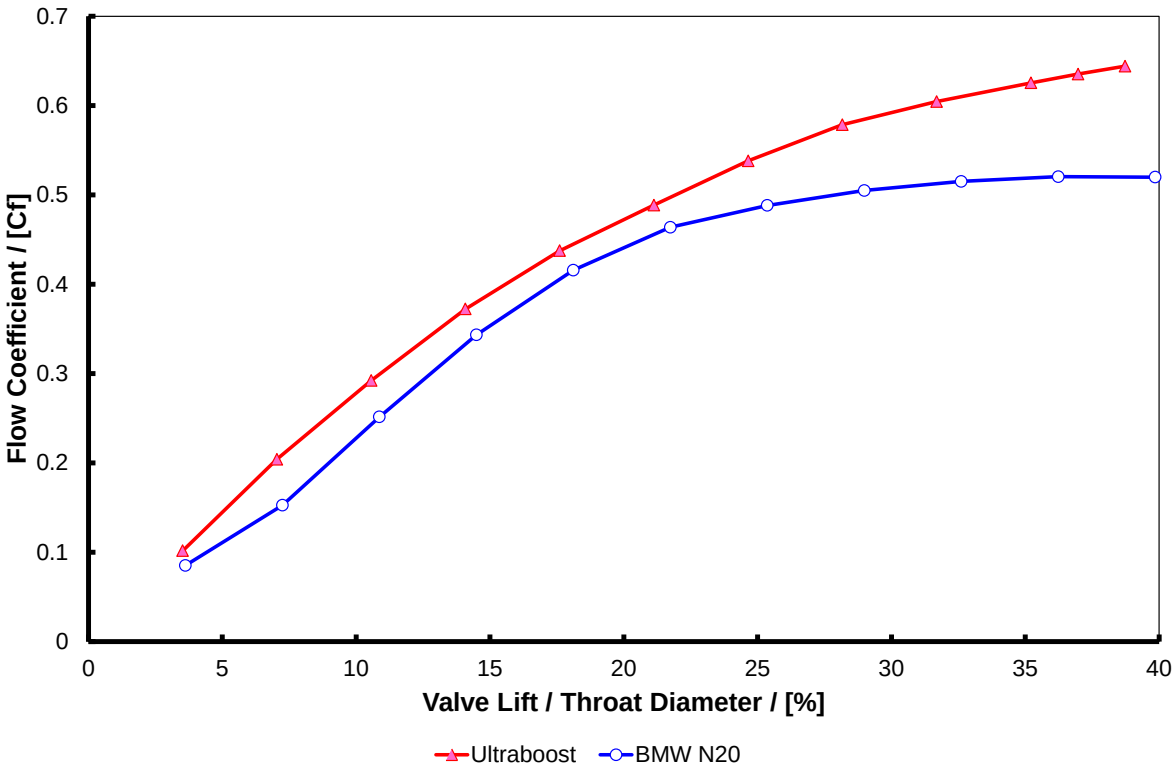

Fig. 5: Inlet port flow coefficient comparison for the Ultraboost Phase 2 and the BMW N20 cylinder heads

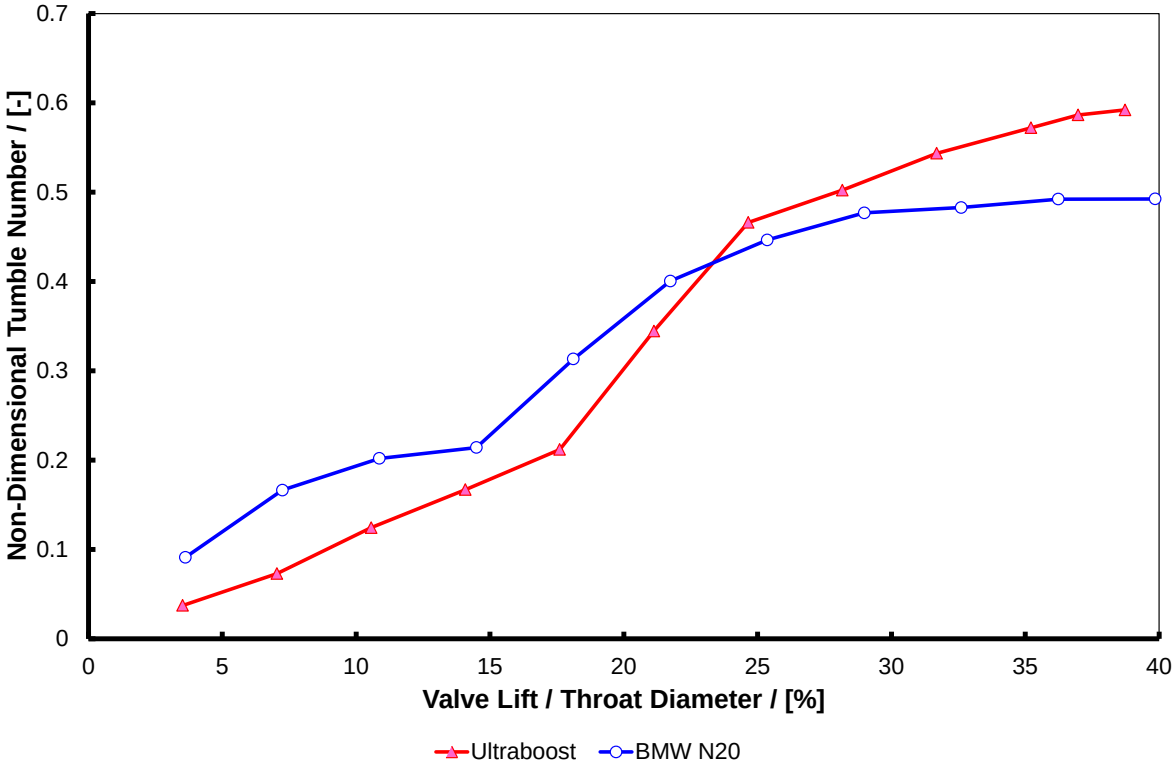

Fig. 6: Inlet port non-dimensional tumble number comparison for the Ultraboost Phase 2 cylinder head and the BMW N20

Conversely, Ultraboost was only ever going to use two-step CPS tappets and the achievement of high outright tumble rates was considered to be paramount, even for part-load operation (where greater in-cylinder air motion would still result when the full valve lift curve was being used, albeit at the expense of relatively higher throttling loss). The use of valve shrouding in the BMW is reflected in the values for the tumble ratio for the two ports, Ultraboost giving 1.626 and the BMW 1.868.

The fact that the Ultraboost port gives high tumble throughout the majority of the effective high-lift cam profile – from 7 mm to 10.5 mm – was considered a success, especially when paired with the high flow coefficient achieved. The effort expended in this part of the project was vindicated by the fact that the port was not changed since it was finalized, the engine being extremely knock tolerant and not suffering from preignition (which, as mentioned previously, would both be expected to benefit from extremely good homogenization of the charge at the time and point of ignition).

5 Engine performance status at end of Phase 2

At the end of the Phase 2 testing, for most of which the CAHU was used, the engine was fitted with the turbocharger and a simple test-bed based air-to-water charge cooler and suitable air pipe work. It was tested in this configuration in order to prove that the turbocharger was capable of providing the maximum power performance demanded and also to establish where its run-up line was in relation to the full-load curve. The results of this test are shown in Figure 7.

A final set of tests was undertaken to look at the effect of charge air temperature within a fixed charge air density regime. This was considered important with regard to combustion effects and to gauge the importance of effective charge cooling on combustion. Since the charge air density was fixed, then, for a fixed relative air-fuel ratio (λ) and level of charge trapping ensured by the valve timing, the chemical energy flowing through the engine would be constant. Any changes in knock-limited spark advance (KLSA) would therefore primarily be due to the change in end-gas temperature- and pressure-time histories arising from the different start-of-compression states. The rationale for the approach has been discussed previously [19,20]. The test was performed because the accuracy of the CAHU unit, with regards to holding target charge air conditions, was previously found to have been extremely good, thus facilitating the approach (the accuracy having been recorded at <0.2% over the range of set-points used throughout engine testing during Phase 2).

Results for this test, in terms of KLSA, are seen in Figure 8. Immediately apparent is that the response to reduced temperature is linear: for each set of constant charge air density data, as the air temperature is reduced (and the air pressure is reduced concomitantly to maintain the fixed density density) KLSA increases monotonically. This is remarkable given the non-linearity of heat transfer effects and combustion kinetics, but the data reinforces earlier research in this area [19,20], albeit at much

higher charge air densities and in a completely different engine. Given the result and its importance, further work in this area is planned for a follow-on project, not least to investigate secondary effects such as the interaction of overlap with scavenging pressure as the air temperature and pressure conditions are changed.

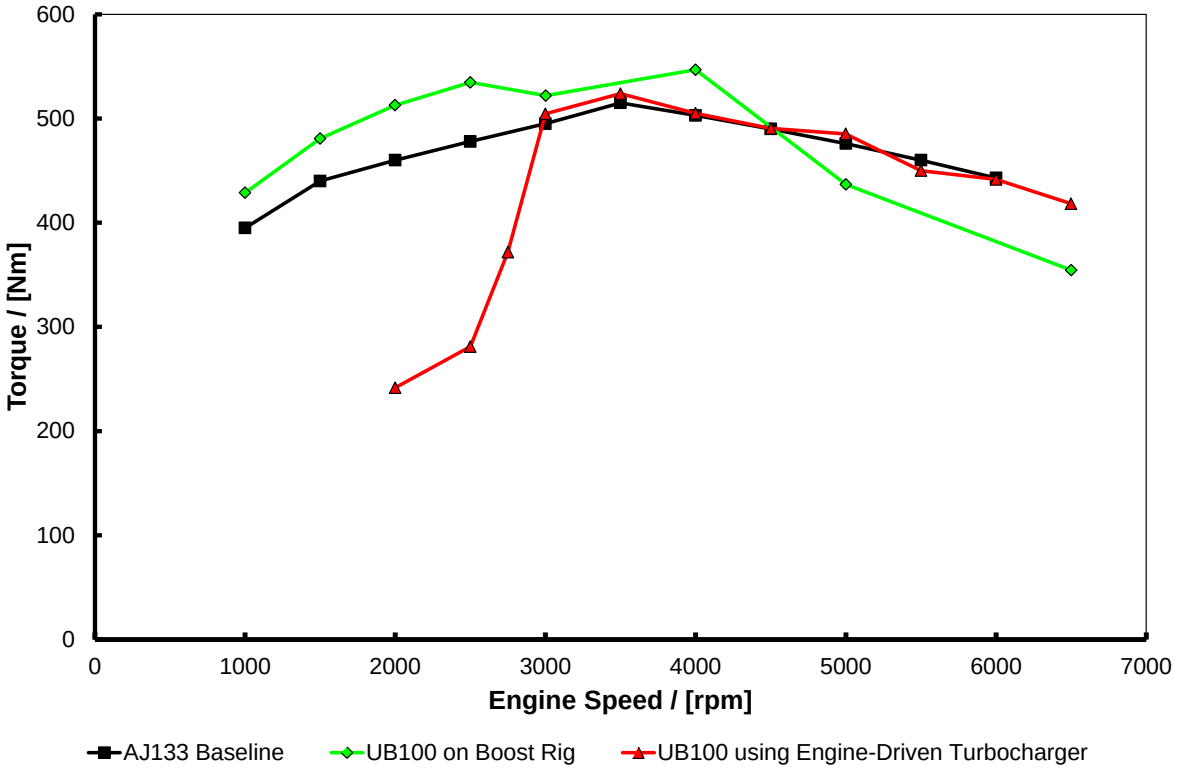

Fig. 7: Engine performance status at end of Phase 2, using UB100 engine and GT30 turbocharger with simple test-bed charge cooling and pipe work

6 UB200 engine performance

For Phase 3, the engine was built to the UB200 specification and was first operated at Lotus Engineering as part of the hot test procedure and EMS commissioning process. It was then shipped to the University of Bath and fitted to the test cell for run-in and testing, as shown in Figure 9.

6.1 Full-load performance

At the time of writing, the full UB200 engine test programme was still under way. The status of the full-load performance at the time is shown in Figure 10. In this figure, the data for the UB200 torque curve represents a combination of UB200 data up to 4750 rpm and the data from Figure 7 from 5000 rpm upwards. This is because it has not yet been possible to operate the engine above 5000 rpm due to the need to fit

wastegate position instrumentation. This situation has not stopped the measurement of part-load data at the points relevant for drive cycle operation (see next section).

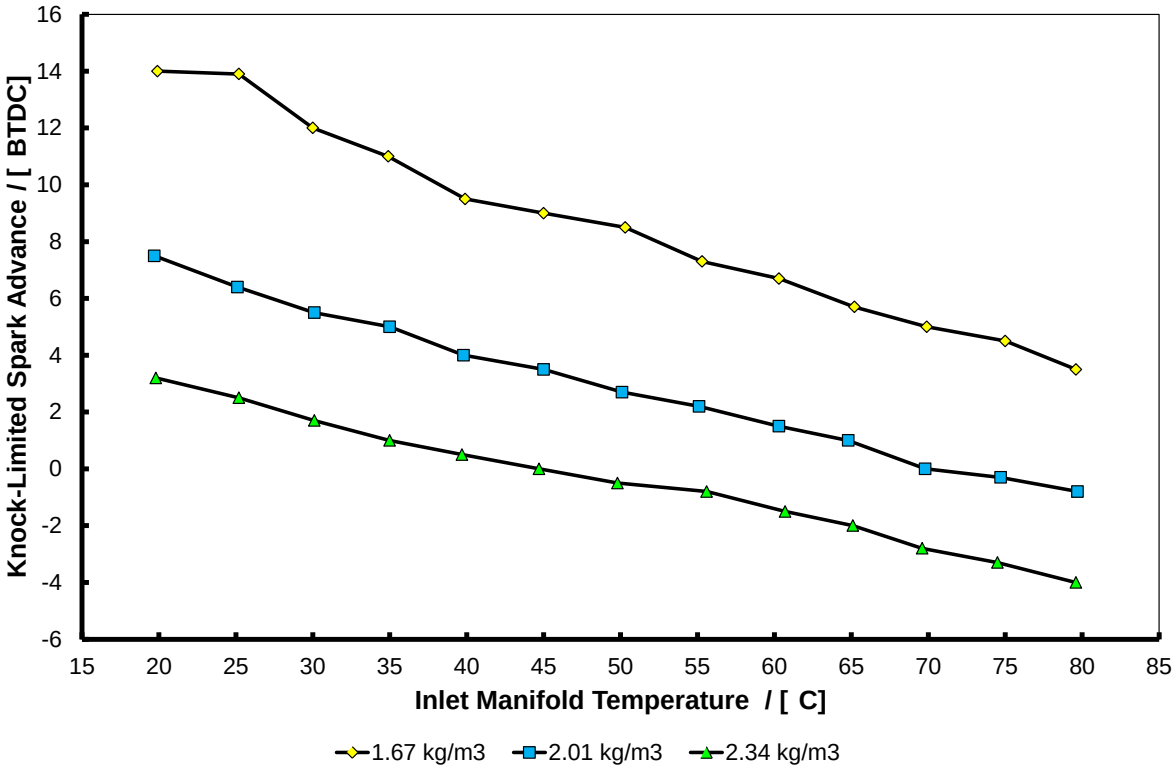

Fig. 8: KLSA versus charge air temperature for constant charge air density tests: UB100 engine operating with CAHU

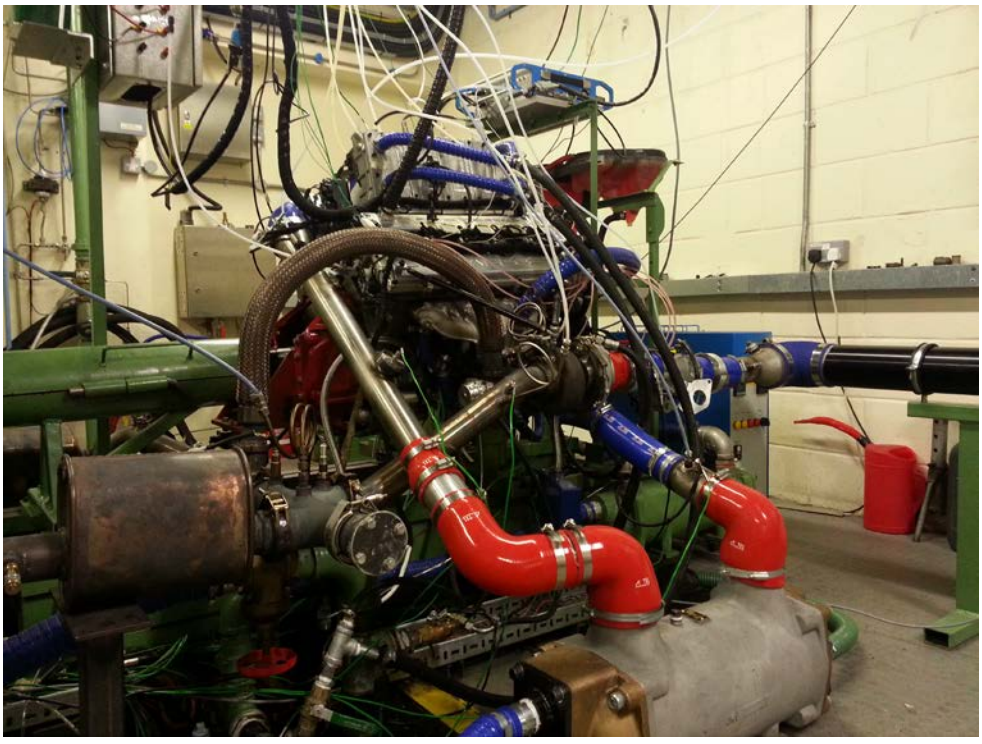

Fig. 9: UB200 engine fitted to the test cell at the University of Bath

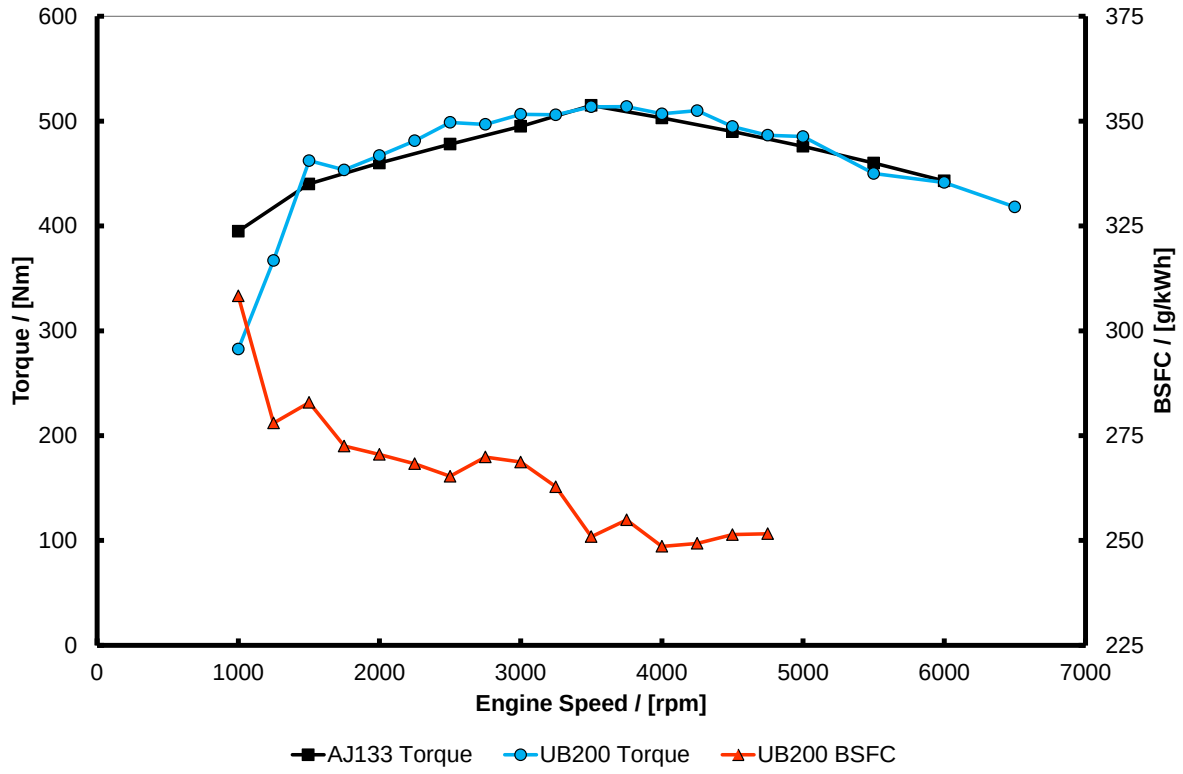

Fig. 10: UB200 full-load performance with 5.9:1 supercharger pulley ratio and 0.8 A/R turbocharger turbine (see text for further explanations)

Immediately apparent in Figure 10 is a shortfall in low-speed torque. The early stages of testing had highlighted this area and a higher supercharger drive pulley ratio of 5.9:1 was procured and fitted for the data presented; the originally-delivered pulley ratio was lower than expected so this modification was merely correcting that state of affairs. However, this low-speed shortfall was also a function of the extremely steep turbocharger run-up line (itself apparent in the earlier tests shown in Figure 7); in the combined supercharger / turbocharger area of operation extremely fine control of wastegate and bypass has been found to be necessary because of the steepness of the run-up curve because overshoot is easily achieved.

In order to improve this situation a turbocharger is being procured with a smaller A/R for the turbine (0.67 versus 0.8 as tested to date), which should enable the target curve to be met with a less-severe build up in boost from the low-pressure stage. Again, this lower A/R ratio was actually the one originally specified but which could not be supplied in the timing required. Further reporting of full-load performance will be reported in later publications.

It should also be pointed out that the large gas-wetted area and very high cooling capacity of the WCEM reduces pre-turbine temperature and enthalpy to a degree greater than would be expected of a fully-optimized integrated exhaust manifold. This has been demonstrated by other researchers [21], where the turbocharger run-up line was delayed by 500 rpm, and in this application this will clearly have a detrimental effect given the observed sensitivity of the charging devices to each

other's performance. Fitting a more-optimized integrated exhaust manifold or a conventional steel component would significantly improve the situation at 1250 rpm and below.

BSFC data is also presented in Figure 10, for the full UB200 build only. The declining contribution of supercharger drive power is readily apparent, up to the point at which the supercharger is clutched out at 3250 rpm. This is due to its bypass being progressively opened as the required contribution to the overall charging system pressure ratio from it reduces. Generally, operating to a pre-turbine temperature of 900°C in the mid-range, the turbocharger-only portion of the BSFC curve is very good (at around 250 g/kWh), despite the high boost pressures demanded; however, it is accepted that this situation may worsen when the new turbine with the lower A/R turbocharger is fitted.

All of the low-speed data presented in Figure 10 was gathered at λ=1 with no cooled EGR being used up to 3500 rpm; the engine is extremely knock-tolerant and does not suffer from pre-ignition, both of which are believed to be due in no small part to the high level of tumble generated by the intake port for its outright flow capability. Between 3750 and 4000 rpm 8% cooled EGR was used and at 4250 and above 10% was utilized. Since it is not used for knock suppression, at the higher speeds the cooled EGR is introduced primarily as a means of reducing exhaust gas temperatures.

At 1250 rpm the engine is producing 367 Nm, representing a BMEP of 23.1 bar. Obviously, the earlier work during Phase 2 of the project had demonstrated that the combustion system is capable of performing above the level required, and when fitted with the turbocharger only the engine had also proved capable of meeting the power target. The later stages of the project will show the final performance status versus the target torque curve.

6.2 Part-load fuel economy

Optimization tests at the 15 minimap points responsible for 99% of fuel consumption on the drive cycle have been conducted. These points and associated results are shown in Figure 11.

Of these results point 7 has the biggest benefit (a reduction in BSFC of 38.1%); it also has the highest residency in the NEDC drive cycle. It is followed by points 8, 2 and 5 (improvements of 36.8%, 29.0% and 18.8%, respectively). Points 11 and 12 are quite highly boosted, with a concomitant amount of supercharger work being required, and so represent a worsening of fuel consumption in comparison to the AJ133 benchmark, but this is lower in magnitude than the benefits seen in the beneficial points (6.4% and 14.7% increase in BSFC, respectively). Points 4 and 6 are also slightly boosted, but still represent a slight improvement (0.3% and 4.4%), indicating that the pumping, thermal and engine friction benefits associated with downsizing can offset extra work in the charging system at some loads.

Minimap Point	Engine Speed (rpm)	Brake Torque (Nm)	BSFC (g/kWhr)	BSFC relative to AJ133 (%)
1	600	27.9	482.4	-35.0
2	1500	39.8	355.1	-29.0
3	1500	104.2	257.7	-13.7
4	1500	198.9	248.1	-0.3
5	2000	79.6	275.2	-18.8
6	2000	198.6	239.3	-4.4
7	1250	15.9	614.5	-38.1
8	1000	15.9	612.9	-36.8
9	1000	79.6	278.5	-17.2
10	1250	159.2	246.7	-6.1
11	1350	238.7	260.5	6.4
12	1500	298.4	273.9	14.7
13	1250	119.4	254.5	-10.7
14	1250	59.7	294.6	-24.7
15	1500	139.3	247.4	-8.4

Fig. 11: UB200 part-load fuel economy at 15 minimap points with 5.9:1 supercharger pulley ratio and 0.8 A/R turbocharger turbine

The data in Figure 11 was input to a proprietary JLR vehicle fuel economy program in order to establish the expected improvement in fuel consumption and CO_2 emissions. The project benchmark vehicle was a production-specification 2010 model year Range Rover fitted with the AJ133 V8 NA engine and 6-speed automatic transmission, without stop-start technology, and this will be used for comparison purposes here. Including all of the idle fuel consumption (see below), the UB200 engine data presented in Figure 11 yields a fuel consumption improvement of 15.0%. In itself this is a significant improvement over the benchmark, because the AJ133 engine was itself designed with best BSFC in mind and also uses short cam profiles and wide-range phasing for throttling loss reduction [6].

At the time of writing, a full optimization of the idle condition had not been completed, so the value given in Figure 11 represents an assumed 35% reduction over AJ133. In terms of weighting in the model, the biggest contribution to overall fuel consumption is from this idle condition. Therefore applying start-stop technology would significantly improve the situation, and removing idle fuel usage in its entirety (to provide a limit case) increases the expected improvement to 23.0%.

The continuing importance of idle fuel consumption is interesting because downsizing makes it a smaller proportion of the total fuel used (due to the reduction of throttling and friction). This fact is illustrated by removing the idle fuelling contribution from the equivalent data for the AJ133 baseline (which was recorded as part of the benchmarking during Phase 1 of the project as discussed above). This alone improves the modelled NEDC fuel consumption of the AJ133-equipped benchmark vehicle by 12.3% (again, a limit case). Applying stop-start is therefore still an extremely beneficial move for the NEDC despite downsizing the engine by 60%.

Directionally, therefore, since light-load conditions still have high residency on the drive cycle even with very highly-downized engines such as this, on an engine level some means of dethrottling the engine further will be advantageous (in addition to stop-start technology). While several of the data gathered for Figure 11 used the low-lift profiles, these represent a single discrete setting and not an optimized time-area solution for Miller cycle operation throughout the map. Future iterations of such engines would still be expected to benefit from continuously-variable valve lift, provided the impact on in-cylinder air motion and any friction demerit can be offset by pumping loss reduction. Such technology interactions have been shown to work on production engines, albeit with a much lower downsizing factor of about 33% [18] (i.e., a 3.0 litre NA engine being replaced with a 2.0 litre turbocharged one). Finally, it is interesting to note that in the case of automatic transmission utilization, because of the downspeeding then possible in normal operation, on a vehicle system level some of the throttling loss reduction may not be realized. Such are the trade-offs in powertrain system selection.

The improvement in fuel consumption presented in Figure 11 is essentially only that attributable to downsizing and the removal of a bank of cylinders. Because of the adoption of the bottom end of the AJ133 engine, the Ultraboost engine still has two high-pressure fuel pumps, a non-adjustable oil pump with flow rate sufficient for a V8, and a mechanical water pump with excess capacity. Since the engine is using exactly the same injectors as the donor engine, there is an argument to say that just one high-pressure pump would suffice. Furthermore, in order to use the fast-acting camshaft phasers from the AJ133, it also has ‘thumper’ cams to provide a non-uniform driving force, which will also increase friction. The AJ133 engine also has an extra shaft for its oil and high-pressure fuel pumps, whose friction is therefore shared between a smaller number of cylinders in Ultraboost. Effectively, the downsized engine is carrying a lot of friction compared to a fully-optimized, clean-sheet design. Given the demonstrated importance of the light-load points on drive-cycle fuel economy, it is intended to investigate the effect of friction in more detail.

The final project aim was to determine the fuel consumption benefit of fitting a heavily-downsized engine in a 2013 Range Rover, when operated on the NEDC. This vehicle is significantly lighter than the 2010 model (by approximately 400 kg), utilizes an 8-speed transmission, and also has stop-start technology. In order to show the result of the various vehicle-level trade-offs, more detailed modelling of the Ultraboost engine in this vehicle is underway in order to gauge how close to the ultimate target of 35% reduction in CO_2 emissions on the NEDC the engine is capable of realizing. These results will be reported in later publications, together with results for other drive cycles.

7 Conclusions

The Ultraboost project is a major collaborative engine research project part-funded by the Technology Strategy Board, the UK's innovation agency. It is led by Jaguar Land Rover with industry- and academia-wide support. It seeks to realize an engine concept downsized by 60% from a naturally-aspirated 5.0 litre V8 engine utilizing production technologies and with attributes suitable for deployment in premium saloons and SUVs. To that end it employs central, close-spaced direct fuel injection, independent cam profile switching and wide-range phasing for the intake and exhaust camshafts. It is fitted with an advanced charging system with two stages of charge air cooling and utilizes low-pressure cooled EGR together with a water-cooled exhaust manifold. Overall, it is designed to withstand peak cylinder pressures of 130 bar.

The intake port was the subject of much investigation and optimization using CFD. It develops very high charge motion for a high mass flow, and its performance is considered fundamental to the preignition resistance of the engine together with its high knock limit.

During Phase 2 of the project it was demonstrated that when the engine was operated using a facilitated charging system the combustion system can deliver the gross BMEP necessary to meet the low-end torque target. It was also shown that the power and torque targets could be met with the selected turbocharger. When operating with a first iteration of the full charging system in Phase 3, a slight shortfall in torque at 1250 rpm and below has been found, but countermeasures are being enacted to mitigate this.

Modelled in a like-for-like manner in a 2010 Range Rover, the engine itself is estimated to be capable of delivering between 15 and 23% improvement in fuel economy on the NEDC, depending on idle fuel consumption. This is despite the engine not being friction-optimized which, for a variety of architectural reasons, would be expected to improve things further. In the target 2013 model year Range Rover with the vehicle level changes that this represents, 35% fuel economy improvement in the target vehicle should be achievable, particularly when the relatively high friction of the engine is taken into account. Later work will discuss the fuel consumption improvements possible on the NEDC and other drive cycles.

8 Acknowledgements

The authors of this paper would like to thank all of the other members of the Ultraboost consortium for their involvement and enthusiasm and the Technology Strategy Board for their continued support, without any of whom this project would not have been possible.

9 Definitions, Acronyms, Abbreviations

ATDC	After top dead centre
BDC	Bottom dead centre
BMEP	Brake mean effective pressure
BTDC	Before top dead centre
CAHU	Combustion air handling unit
CPS	Cam profile switching
CFM	Cubic feet per minute
DCVCP	Dual continuously-variable camshaft phasing
DF	Downsizing factor
DI	Direct injection
EAT	Exhaust after treatment
EGR	Exhaust gas recirculation
IEM	Integrated exhaust manifold
IMEP	Indicated mean effective pressure
JLR	Jaguar Land Rover
KLSA	Knock-limited spark advance
MOP	Maximum opening point
NA	Naturally aspirated
NEDC	New European Drive Cycle
SI	Spark ignition
TDC	Top dead centre
UB	Ultraboost (Ultra Boost for Economy)
V_{Swept}	Swept volume
WCEM	Water-cooled exhaust manifold
η_{mech}	Mechanical efficiency

10 References

[1] HEYWOOD, J.B.
Internal Combustion Engine Fundamentals
McGraw-Hill Book Company, New York, USA, 1988, ISBN 0-07-100499-8

[2] COLTMAN, D., TURNER, J.W.G., CURTIS, R., BLAKE, D., HOLLAND, B., PEARSON, R.J., ARDEN., A., NUGLISCH, H.
Project Sabre: A Close-Spaced Direct Injection 3-Cylinder Engine with Synergistic Technologies to achieve Low CO_2 Output
SAE paper number 2008-01-0138, SAE Int. J. Engines 1(1):129-146, 2009, doi:10.4271/2008-01-0138
SAE 2008 World Congress
Detroit, Michigan, USA, 14th-17th April, 2008

[3] KREBS, R., SZENGEL, R., MIDDENDORF, H., FLEIß, M., LAUMANN, A., VOELTZ, S.
The New Dual-Charged FSI Petrol Engine by Volkswagen Part 1: Design
MTZ 11/2005, Volume 66, pp. 2-7

[4] ANDRIESSE, D., COMIGNAGHI, E., LUCIGNANO, G.., OREGGIONI, A., QUINTO, S., SACCO, D.
The New 1.8 l DI Turbo-Jet Gasoline Engine from Fiat Powertrain Technologies
17th Aachen Colloquium, pp. 563-590
Aachen, Germany, 6th-8th October, 2008

[5] HANCOCK, D., FRASER, N., JEREMY, M., SYKES, R., BLAXILL, H.
A New 3 Cylinder 1.2l Advanced Downsizing Technology Demonstrator Engine
SAE paper number 2008-01-0611, doi:10.4271/2008-01-0611
SAE 2008 World Congress
Detroit, Michigan, USA, 14th-17th April, 2008

[6] SANDFORD, M., PAGE, G., CRAWFORD, P.
The All New AJV8
SAE paper number 2009-01-1060, doi:10.4271/2009-01-1060
SAE 2009 World Congress
Detroit, Michigan, USA, 20th-23rd April, 2009

[7] McALLISTER, M.J., BUCKLEY D.J.
Future gasoline engine downsizing technologies - CO_2 improvements and engine design considerations
Paper number C684/018, pp. 19-26
Institution of Mechanical Engineers Internal Combustion Engines Conference
London, UK, 8th-9th December, 2009

[8] SALAMON, C., McALLISTER, M., ROBINSON, R., RICHARDSON, S., MARTINEZ-BOTAS, R., ROMAGNOLI, A., COPELAND, C., TURNER, J.W.G.
Improving Fuel Economy by 35% through combined Turbo and Supercharging on a Spark Ignition Engine
21st Aachen Colloquium, pp. 1317-1346
Aachen, Germany, 8th-10th October, 2012

[9] COPELAND, C., MARTINEZ-BOTAS, F., TURNER, J.W.G., PEARSON, R., LUARD, N., CAREY, C,. RICHARDSON, S., di MARTINO, P., CHOBOLA, P.
Boost System Selection for a Heavily Downsized Spark Ignition Prototype Engine
Institution of Mechanical Engineers 10th International Conference on Turbochargers and Turbocharging
London, UK, 15th-16th May, 2012

[10] DAHNZ, C., HAN, K.-M., SPICHER, U., MAGAR, M., SCHIEßL, R., MASS, U.
Investigations on Pre-Ignition in Highly Supercharged SI Engines
SAE paper number 2010-01-0355, doi:10.4271/2010-01-0355
SAE 2010 World Congress, Detroit
Michigan, USA, 13th-15th April, 2010

[11] ZAHDEH, A., ROTHENBERGER. P., NGUYEN, A., ANBARASU, M., SCHMUCK-SOLDAN, S., SCHAEFER, J., GOEBEL, T.
Fundamental Approach to Investigate Pre-Ignition in Boosted SI Engines
SAE paper number 2011-01-0340 and SAE Int. J. Engines 4(1):246-273, 2011, doi:10.4271/2011-01-0340
SAE 2011 World Congress
Detroit, Michigan, USA, 12th-14th April, 2011

[12] PALAVEEV, S., SPICHER, U., MAGAR, M., MASS, U., SCHIEßL, R., KUBACH, H.
Premature Flame Initiation in a Turbocharged DISI Engine - Numerical and Experimental Investigations
SAE paper number 2013-01-0252 and SAE Int. J. Engines 6(1):2013, doi:10.4271/2013-01-0252
SAE 2013 World Congress
Detroit, Michigan, USA, 16th-18th April, 2013

[13] HELDUK, T., DORNHÖFER, R., EISER, A., GRIGO, M., PELZER, A., WURMS, R.
The new generation of the R4 TFSI engine from Audi
32nd Vienna Motor Symposium
Vienna, Austria, 5th-6th May, 2011

[14] ERNST, R., FRIEDFELDT, R., LAMB, S., LLOYD-THOMAS, D., PHLIPS, P., RUSSELL, R., ZENNER, T.
The New 3 Cylinder 1.0L Gasoline Direct Injection Turbo Engine from Ford
20th Aachen Colloquium
Aachen, Germany, 11th-12th October, 2011, pp. 53-72.

[15] TURNER, J.W.G., PEARSON, R.J., CURTIS, R., HOLLAND B.
Improving Fuel Economy in a Turbocharged DISI Engine Already Employing Integrated Exhaust Manifold Technology and Variable Valve Timing
SAE paper number 2008-01-2449, doi:10.4271/2008-01-2449
SAE International Powertrain Fuels and Lubricants Meeting
Rosemont, Illinois, USA, 7th-9th October, 2008

[16] RANINI, A., MONNIER, G.
Turbocharging a Gasoline Direct Injection Engine
SAE paper number 2001-01-0736, doi:10.4271/2001-01-0736
SAE 2001 World Congress
Detroit, Michigan, USA, 5th-8th March, 2001

[17] BANDEL, W., FRAIDL, G.K., KAPUS, P., SIKINGER, H., COWLAND, C.N.
The Turbocharged GDI Engine: Boosted Synergies for High Fuel Economy Plus Ultra-low Emissions
SAE paper number 2006-01-1266, doi:10.4271/2006-01-1266
SAE 2006 World Congress
Detroit, Michigan, USA, 3rd-6th April, 2006

[18] STEINPARZER, F., UNGER, H., BRÜNER, T., KANNENBERG, D.
The new BMW 2.0 litre 4-cylinder S.I. engine with Twin Power Turbo Technology
32nd Vienna Motor Symposium
Vienna, Austria, 5th-6th May, 2011

[19] TURNER, J.W.G., PEARSON, R.J., MILOVANOVIC, N., TAITT, D.
Extending the knock limit of a turbocharged gasoline engine via turboexpansion
Institution of Mechanical Engineers 8th International Conference on Turbochargers and Turbocharging
London, UK, 17th-18th May, 2006

[20] TURNER, J.W.G.
Interactions Between Charge Conditioning, Knock and Spark-Ignition Engine Architecture
Loughborough University
Loughborough, UK, April 2011

[21] TAYLOR, J., FRASER, N., WIESKE, P.
Water Cooled Exhaust Manifold and Full Load EGR Technology applied to a Downsized Direct Injection Spark Ignition Engine
SAE paper number 2010-01-0356, doi: 10.4271/2010-01-0356
SAE 2010 World Congress
Detroit, Michigan, USA, 12th-14th April, 2010